Dewetting on porous media with aspiration

A. Aradian[a], E. Raphaël[b], and P.G. de Gennes[c]

Physique de la Matière Condensée[d], Collège de France, 11 place Marcelin Berthelot, 75231 Paris Cedex 05, France

Abstract. We consider a porous solid covered with a water film (or with a drop) in situations where the liquid is pumped in, either spontaneously (if the porous medium is hydrophilic) or mechanically (by an external pump). The dynamics of dewetting is then strongly modified. We analyse a few major examples, a) horizontal films, which break at a certain critical thickness, b) the "modified Landau-Levich problem" where a porous plate moves up from a bath and carries a film: aspiration towards the plate limits the height H reached by the film, c) certain situation where the hysteresis of contact angles is important.

PACS. 68.45.Gd Wetting – 68.15.+e Liquid thin films – 81.05.Rm Porous materials; granular materials

1 General aims

The current picture of dewetting processes on flat, smooth surfaces is relatively clear [1], although inertial regimes still raise some questions [2]. But if the surface is porous, the situation is very different. A number of practical problems belong to this class:

i) In the 4-color offset printing, a sheet of paper may be at one moment covered by a water film. The water must be removed very fast when the sheet reaches the desired printing roller: this dewetting process is assisted by a spontaneous suction of the water into the hydrophilic paper [3].

ii) Many industrial processes involve the rapid passage of a solid film, into a liquid bath. When the film leaves the bath, it drags a Landau-Levich film [4,5]. However, if the film is porous, and sucks in the fluid, there is a height H at which the Landau-Levich film disappears: what is the value of H? [6].

iii) When we paint with a brush, we are in fact transferring a liquid from a porous medium onto a flat surface—the reverse process.

Our aim, in the present text is not to cover all these complex systems, but to choose a few model examples where the effects of aspiration (towards the solid) are non-trivial. The essential parameter describing the aspiration is the normal current J (volume/unit area/unit time). When we pump through a given thickness of porous solid, with a prescribed pressure drop, J is controlled by Darcy's law. When we have a spontaneous suction, over a time interval t, J is related to the Washburn equation [7]: the

scaling structure of J (for a pore volume fraction $\sim 1/2$ and wetting angles $\sim 1\,\mathrm{radian}$) is simply

$$J \simeq \left(\frac{D}{t}\right)^{1/2}. \tag{1}$$

In equation (1), the parameter D has the dimensions of a diffusion coefficient:

$$D = \frac{\gamma}{\eta}d \equiv V^*d, \tag{2}$$

where d is the pore diameter, γ is the surface tension, η the viscosity of the fluid, and $V^* = \gamma/\eta$ is a characteristic capillary velocity. In all the model systems to be discussed below, we shall assume that J is prescribed and is time independent. (One case where the time dependence may matter is discussed in Ref. [6]). We also assume that the pore diameter d is very small: then we may describe the capillary hydrodynamics in a continuous picture.

One natural feature of a porous surface is to pin down a contact line—*i.e.* to bring in a certain hysteresis in the contact angles. If the equilibrium value of this angle (as given by Young's law) is θ_e, the receding angle is $\theta_\mathrm{r} < \theta_\mathrm{e}$. Two distinct cases can be found in practice:

a) "strong" pinning $\theta_\mathrm{r} = 0$;
b) "weak" pinning $\theta_\mathrm{r} > 0$.

In this paper, we start (Sects. 2 and 3) by a discussion of pumping effects on surfaces with no hysteresis[1]: this is

---

[a] e-mail: `Achod.Aradian@college-de-france.fr`
[b] e-mail: `Elie.Raphael@college-de-france.fr`
[c] e-mail: `Pierre-Gilles.deGennes@espci.fr`
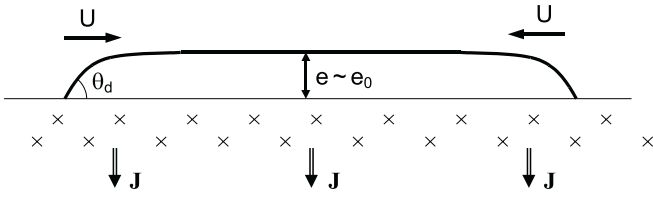[d] URA 792 du C.N.R.S.

[1] In order to have a good determination of the thermodynamic angle θ_e, we do not necessarily need an ideal surface without defects. As shown by J.F. Joanny and P.G. de Gennes (J. Chem. Phys. **81**, 552 (1984)) in the case of "regular" defects, we need only a surface with irregularities below a certain strength threshold. In Sections 2 and 3, the local dissipation which might be associated to these defects is assumed to be negligible.

Fig. 1. Macroscopic puddle under aspiration.

not usual, but conceptually important. We then proceed to some cases of hysteresis inducing weak or strong pinning.

In Section 2, we consider horizontal films, which thin out and become unstable at a certain critical thickness. Then we proceed in Section 3 towards vertical plates pulled out of a liquid: the modified Landau-Levich problem. In Section 4, we allow for hysteresis, first solving the macroscopic problem of a pinned drop, then reconsidering the vertical plate situation. Section 5 discusses some possible extensions and some limitations of the present work.

2 Horizontal films

2.1 A macroscopic puddle under aspiration

This case is described in Figure 1. It has been studied recently theoretically and experimentally by Bacri and Brochard [8]. Here we present only the case with no hysteresis, because it provides a good introduction.

Let us denote by S the spreading parameter $\gamma_{SO} - (\gamma + \gamma_{SL})$, where γ is the liquid surface tension, and γ_{SL} (respectively, γ_{SO}) the interfacial tension of the wet (respectively, dry) solid. We assume S to be negative (partial wetting). The equilibrium puddle has a thickness e_0 which results from a balance between gravity (tending to decrease e_0) and capillarity (struggling for a minimal exposed area). For a large puddle (radius $R \gg e_0$) on a partially wettable substrate, this corresponds to the following energy:

$$f = \frac{1}{2}\rho g e^2 \frac{\Omega}{e} + \frac{\Omega}{e}\big(\gamma + \gamma_{SL} - \gamma_{SO}\big), \qquad (3)$$

where Ω is the liquid volume, Ω/e the contact area, ρ the density, and g the gravitational acceleration. Minimizing (3) with respect to e gives a classic formula for e_0 (which is typically of order 1 mm) [9]:

$$e_0 = \sqrt{2\frac{-S}{\rho g}}. \qquad (4)$$

Let us now pump on this structure, imposing a *small* current J (and assuming zero hysteresis). Then e remains close to e_0. The horizontal shrinkage velocity U is related to J by the conservation equation:

$$2\pi R e_0 U = \pi R^2 J, \qquad (5)$$

from which we deduce

$$U = J\frac{R}{2e_0}. \qquad (6)$$

All the structure is slightly distorted. For instance the dynamic contact angle θ_d is slightly smaller than θ_e, because there is a Poiseuille flow in the vicinity of the contact line. The necessity for this flow can be perceived starting from the opposite assumption: if the liquid in the puddle was flowing downwards, uniformly with velocity J, the lateral velocity, deduced from the position of the contact line, would be $\tilde{U} = J/\theta_e \neq U$. We can estimate the difference $\theta_e - \theta_d$ from a standard dissipation argument [1]:

$$T\overset{\bullet}{\Sigma} = \frac{3\eta}{\theta_d}\big(U - \tilde{U}\big)^2 \log\frac{e_0}{\theta_d a} = $$
$$(U - \tilde{U})\gamma\big(\cos\theta_d - \cos\theta_e\big) \qquad (7)$$

(where we have assumed θ_e and θ_d to be small, since this is the most universal case). The argument in the logarithm is the size $\sim e_0/\theta_d$ of the Poiseuille region (near the rim), divided by a molecular length.

2.2 Nanoscopic pancakes or films

We now pump on a very thin film (e = nanometers), and assume first that the solid surface is partly wettable (*i.e.* $\gamma_{SO} < \gamma_{SL} + \gamma$). At these small scales, the film energy $F(e)$ per unit area can be written as [10]

$$F(e) = \gamma_{SL} + \gamma + P(e), \qquad (8)$$

where, for e much larger than the molecular size a_0, $P(e)$ is controlled by long-range van der Waals forces[2]:

$$P(e) = \frac{A}{12\pi e^2} \quad (e \gg a_0). \qquad (9)$$

We will assume that the Hamaker constant A is positive. For shorter distances ($e \gtrsim a_0$), the precise form of $P(e)$ is generally unknown, but in the limit $e \to 0$, we have $P(e \to 0) = \gamma_{SO} - \gamma - \gamma_{SL}$ since we must recover $F = \gamma_{SO}$ (dry solid). The general aspect of $F(e)$ for partial wetting is shown in Figure 2a.

As long as the curvature $F''(e)$ is positive, our film is either stable or metastable [11]. In the case of Figure 2a, for a thickness e larger than a certain thickness e_s such that $F''(e_s) = 0$, the film is metastable [12]. Thus, in the absence of dry patch nucleation, we can get down without changes to e_s. But, when e reaches e_s, a spinodal decomposition is expected [12]. If we stopped the pumping at this moment, this would ultimately lead to a coexistence between dry regions and finite, macroscopic droplets. But if we persist in pumping, the early droplets (of thickness $\sim e_s$) will fade out before any major coalescence process.

A similar discussion can be given for the case of complete wetting ($\gamma_{SO} > \gamma_{SL} + \gamma$). The corresponding plot of $F(e)$ is pictured in Figure 2b. In the absence of pumping, the liquid forms a "pancake" of *nanoscopic* thickness $e = e_p$. The equilibrium condition determining e_p is [9]

$$e_p \Pi(e_p) + P(e_p) = S, \qquad (10)$$

---

[2] We only retain non-retarded van der Waals interactions: the retarded regime occurs for distances larger than those that will be considered in this paper.
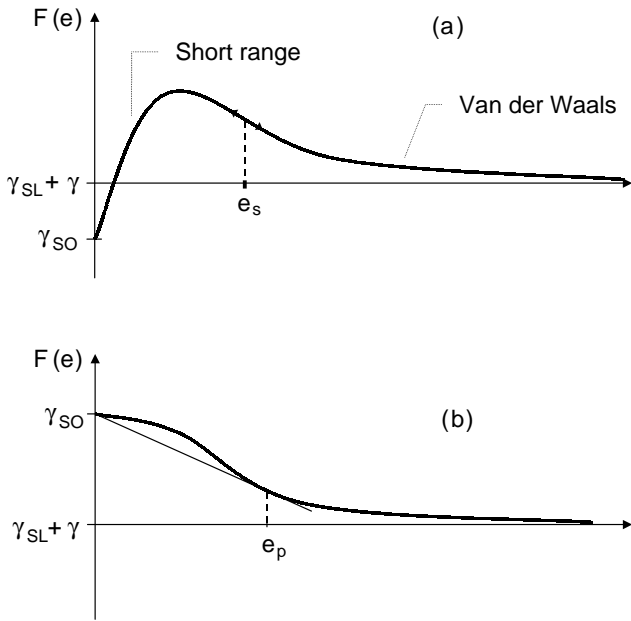
Fig. 2. Film energy *versus* film thickness in the case of: (a) partial wetting, (b) complete wetting.

where $\Pi(e) \equiv -\partial P/\partial e$. Equation (10) may be interpreted as a balance of forces on the contact line: the Young force $S = \gamma_{\rm SO} - (\gamma_{\rm SL} + \gamma)$ is equilibrated by the pressure due to van der Waals attractions. (The graphical construction of $e_{\rm p}$ is shown in Figure 2b: $e_{\rm p}$ is the point for which the tangent to $F(e)$ intercepts the vertical axis at $\gamma_{\rm SO}$).

As a consequence of this, when pumped, a continuous film would tend, at $e < e'_{\rm s}$ (where $F''(e'_{\rm s}) = 0$), to break into a mixture of such pancakes and dry regions rather than thin further out uniformly. Each pancake will then shrink by a process reminiscent of the puddle (*e.g.*, Eq. (5)).

Of course, all this discussion of nanoscopic objects is rather unrealistic, since most porous media have pores larger than the structure described here: our continuum description can be adequate only if our porous surface was based on an extreme permeation membrane, with pore diameters of a few angstroms! But, in spite of this strong limitation, the discussion is (we think) conceptually helpful.

3 The modified Landau-Levich problem

3.1 A reminder on nonporous systems

We pull out a vertical plate from a bath (Fig. 3a) at velocity V. If the plate is partially wettable (equilibrium contact angle $\theta_{\rm e}$), and the velocity V is very low, we retain a dynamic contact angle $\theta_{\rm d}$ close to $\theta_{\rm e}$. If we increase the velocity V, we have a non-trivial relation $V(\theta_{\rm d})$. Of course $V(\theta_{\rm d})$ vanishes at $\theta_{\rm d} = \theta_{\rm e}$, but V also vanishes at $\theta_{\rm d} \to 0$, because the dissipation in a thin wedge is very large. The simplest (crudest) form, valid for small angles,
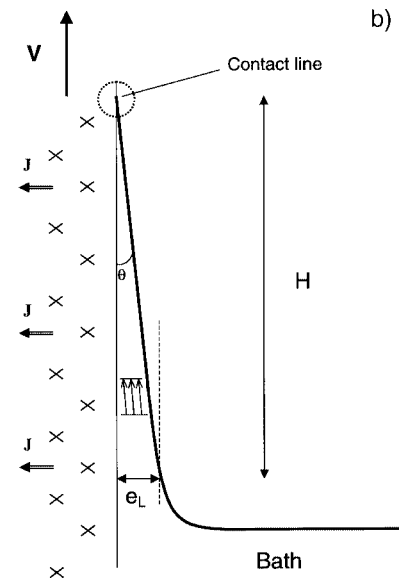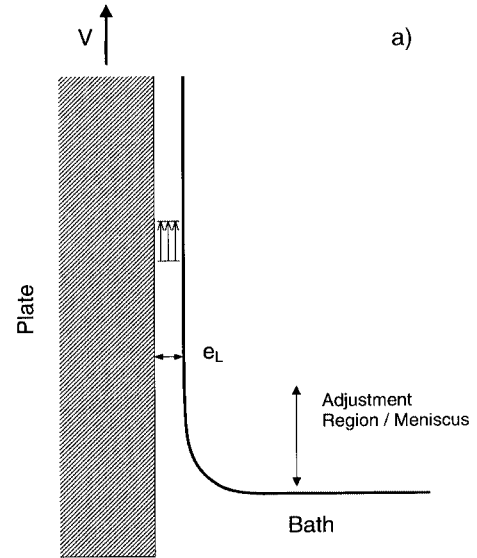
Fig. 3. Pull out at velocity V of a vertical plate from a bath: a) The classic Landau-Levich problem. b) The modified Landau-Levich problem, with a porous plate inducing an aspiration current J. Most of the film then displays a tilted profile of angle $\theta = J/V$, with a plug flow velocity field, and terminates at a height $H = e_{\rm L}/\theta$. In the present article, we investigate the microscopic structure of the film near the contact line (region inside the dotted circle).

is [1]

$$V(\theta_{\rm d}) = {\rm const}\, V^*\bigl(\theta_{\rm e}^2 - \theta_{\rm d}^2\bigr)\theta_{\rm d}. \qquad (11)$$

This has a maximum

$$V = V_{\rm m} = {\rm const}\, V^*\theta_{\rm e}^3. \qquad (12)$$

If we impose a velocity larger than $V_{\rm m}$ (as usual in fast technical processes) we cannot retain a contact line:

the plate drags with it a film of finite thickness e_L. This thickness was computed in a classic paper by Landau and Levich [4] (for viscous regimes):

$$e_L = b \left(\frac{V}{V^*} \right)^{2/3},\qquad(13)$$

where b is related to the curvature of the underlying meniscus ($b \sim 1\,\mathrm{mm}$). The height of the adjustment region (beyond which the film becomes uniform) is of order $b(V/V^*)^{1/3}$.

The above results for the film thickness and the adjustment region are also valid for a completely wettable plate. In that case, however, there is no velocity threshold and the plate drags a film as soon as $V > 0$.

Equation (13) has been amply verified, and extended up to inertial regimes [5]. Our aim here is to see how the film is modified under pumping, in a viscous regime of small capillary numbers ($Ca = V/V^* \ll 1$).

3.2 Pull out of a surface under pumping: Macroscopic flow

We now consider the pull-out of a substrate able to suck liquid in as it drags a film from the bath. This *modified* Landau-Levich problem was discussed in a simplified form in reference [6], and, for completeness, we start by a brief summary of the main results.

Let us assume that we impose a uniform pumping current J on the film, J being small compared to the drag velocity V. The aspect of the flow is pictured in Figure 3b): as in the usual Landau-Levich film, there is a meniscus from the bath and an adjustment region leading to a thickness e_L. But then on, aspiration comes into play, and we expect that most of the film will have a simple hydrodynamic flow (plug flow) in the external film, without any pressure gradients, where the flow lines are just tilted by the angle $\theta = J/V \ll 1$. As a consequence, the Landau-Levich film thins out and ultimately disappears at a finite height $H = e_L/\theta$.

However the validity of this non-dissipative solution is necessarily restricted to macroscopic scales, and is not acceptable very close to the contact line, where one must take into account local wetting properties such as the spreading parameter S: the slope of the profile must change. It is our aim in the rest of this section to understand the structure of the film in the vicinity of the contact line, both in the case of complete ($S \geq 0$) and partial wetting ($S < 0$).

3.3 Hydrodynamic equation and boundary conditions

Let us denote z the vertical distance measured downwards from the contact line. In the lubrication approximation, we can describe the velocity in the film (in the z-direction) by the following parabolic form:

$$v_z(x) = -V + \frac{V_1}{e^2}(x^2 - 2ex),\qquad(14)$$

dictated by the no-slip condition on the plate, and the absence of tangential stress at the free surface (note that in this formula, V_1 and e are functions of z).

For a steady-state situation, conservation imposes that the upwards flow rate $-\int_0^e v_z(x)\,\mathrm{d}x$ at height z balances the amount Jz of liquid that disappears above due to the pumping:

$$Jz = -\int_0^e v_z(x)\,\mathrm{d}x = e\left(V + \frac{2}{3}V_1\right).\qquad(15)$$

The Poiseuille flow (14) is driven by a pressure gradient $\partial p/\partial z$, where p contains contributions from capillarity and van der Waals forces

$$p = -\gamma\frac{\partial^2 e}{\partial z^2} - \frac{A}{6\pi e^3},\qquad(16)$$

and A is a Hamaker constant.

Writing

$$\frac{\partial p}{\partial z} = \eta\frac{\partial^2 v_z}{\partial x^2} = \frac{2\eta V_1}{e^2},\qquad(17)$$

equation (15) can be rewritten as

$$1 - \frac{\theta z}{e} = \frac{e^2}{3\eta V}\left\{ \gamma\frac{\mathrm{d}^3 e}{\mathrm{d}z^3} + \frac{\mathrm{d}}{\mathrm{d}z}\left(\frac{A}{6\pi e^3} \right) \right\},\qquad(18)$$

where, as before, $\theta = J/V$ is a small angle ($\theta \ll 1$).

Equation (18) is reminiscent of the equation discussed in reference [9] for precursor films over a wettable surface, and in reference [13] for an advancing liquid on a partly wettable surface. But there are two differences: a) pumping introduces a new term ($-\theta z/e$) on the left-hand side, b) the direction of the driving velocity V is reversed (in the frame of the plate, the liquid front moves back).

In order to single out the physical solution of equation (18), it is necessary to impose the three following boundary conditions:

$$\mathrm{i)}\quad e(z) = 0, \quad \mathrm{at}\quad z = 0,\qquad(19)$$

$$\mathrm{ii)}\quad \lim_{z\to 0}\frac{A}{12\pi e(z)^2} - \frac{1}{2}\gamma e'(z) = S,\qquad(20)$$

$$\mathrm{iii)}\quad e \text{ reaches a linear profile when } z\to +\infty.\qquad(21)$$

The boundary condition ii) reflects the local balance of forces on the contact line [9]. Since it involves the spreading parameter S, it will introduce a distinction between situations of total wetting ($S \geq 0$) and situations of partial wetting ($S < 0$).

Far from the contact line, as expected, the profile merges into the macroscopic profile of angle θ described in the previous section: in equation (18), for large thicknesses and vanishing curvature, $e \sim \theta z + c$ is easily seen to be the asymptotic profile (c a constant). But a more thorough analysis of the asymptotic behaviour of equation (18) [14] shows that any profile of angle θ is *not* convenient, and that we must necessarily set $c = 0$. Hence, remarkably enough, if the asymptotic profile were known with sufficient accuracy, by a straight extrapolation of it one could

guess the actual microscopic position of the contact line, regardless of any complicated local behaviour.

Bearing this essential fact in mind, we now turn to solving equation (18) in the case of a completely wettable substrate.

3.4 Wettable surface

We first consider the modified Landau-Levich problem on a wettable surface. From now on, to make later explanations clearer, the two terms of the l.h.s. of equation (18) will be respectively referred to as the "dynamic term"[3] and the "aspiration term", and the terms on the r.h.s., respectively, as "capillary" and "VW" (van der Waals) terms.

We start from the "far-field" region and look for characteristic lengths to scale equation (18). In these scales, we need both the dynamic and aspiration terms to be of order one (to give rise to the asymptotic profile of angle θ), plus a third term to describe the departure from it. One can show that the only consistent choice is to keep the VW contribution of order one. This imposes the following scalings:

$$z_1 = z/\mu_1, \quad \text{with} \quad \mu_1 = \ell, \tag{22}$$
$$e_1 = e/\lambda_1, \quad \text{with} \quad \lambda_1 = \theta\ell, \tag{23}$$

where ℓ is a crucial length of the problem defined by

$$\ell = a\left(\frac{V^*}{J}\right)^{1/2} \tag{24}$$

and a an atomic length (of a few Å) defined as $a^2 = (A/6\pi\gamma)$. We note that ℓ, though much greater than a, remains in the microscopic domain ($J/V^* = 10^{-4}$ gives a few hundred Å).

Our central equation (18) rewrites in these scaled variables

$$1 - \frac{z_1}{e_1} = \epsilon e_1^2 e_1''' - \frac{e_1'}{e_1^2}, \tag{25}$$

where

$$\epsilon = \frac{1}{3}\frac{V^*\theta^3}{V} \tag{26}$$

is a small parameter of the problem[4]: $\epsilon \ll 1$. We thus see that in these scales, capillarity appears as a perturbative term to a behaviour ruled mainly by the pull-out velocity, aspiration and VW. However, we immediately notice that the capillary term, though of order ϵ, contains the highest derivative in the equation, implying that we are in the presence of a *singular perturbation* problem.

---

[3] Since the presence of the "1" in the equation is the direct consequence of the pull-out.

[4] For instance, taking $\theta = 10^{-2}$, $V = 0.7\,\text{m s}^{-1}$ and $V^* = 70\,\text{m s}^{-1}$, gives $\epsilon \simeq 3 \cdot 10^{-5}$.

Such problems have the interesting property that even for arbitrary small ϵ, there always is a region, called *inner* region or *boundary layer*, where the true solution dramatically differs from the simple $\epsilon = 0$ solution[5] (usually named *outer* solution). For the interested reader, extensive coverage of this subject can be found in references [15–18]. In the following presentation, we will try to emphasize physical content rather than enter into technical developments [14].

In our problem, the inner region stands near the contact line, at $z = 0$, and capillarity is called to play an important role there. The outer region, on the other hand, extends from the limit of the inner region (crudely) to infinity.

The (first-order) outer solution is looked for by setting $\epsilon = 0$ in equation (25). We obtain the exact form

$$e_{1,\text{out}} = \frac{e^{z_1^2/2}}{K + \int_0^{z_1} e^{y^2/2}\,\mathrm{d}y}, \tag{27}$$

where K is a constant that will be determined later by matching with the inner solution. One can check that this outer solution respects the asymptotic boundary condition (21).

In the inner region, the essence of singular perturbation techniques is to rescale the independent variable with the help of a power of ϵ in order to change the dominant balance of the equation. Guided by the form of the boundary condition (20) which balances capillarity and VW at the contact line, we choose the following new variables:

$$z_2 = z/\mu_2, \quad \text{with} \quad \mu_2 = \epsilon^{1/2}\ell, \tag{28}$$
$$e_2 = e/\lambda_2, \quad \text{with} \quad \lambda_2 = \lambda_1. \tag{29}$$

The expression of μ_2 reveals that the boundary-layer near the contact line extends over a distance of order $\epsilon^{1/2}\ell$.

In these inner variables, equation (18) takes the inner form

$$\epsilon^{1/2} - \epsilon\frac{z_2}{e_2} = e_2^2 e_2''' - \frac{e_2'}{e_2^2}, \tag{30}$$

where the dynamic term and the aspiration term remain small, and the behaviour is dictated mainly by a balance between capillarity and VW. Solving to first order (by setting $\epsilon = 0$, and integrating twice), we get z_2 as a function of e_2:
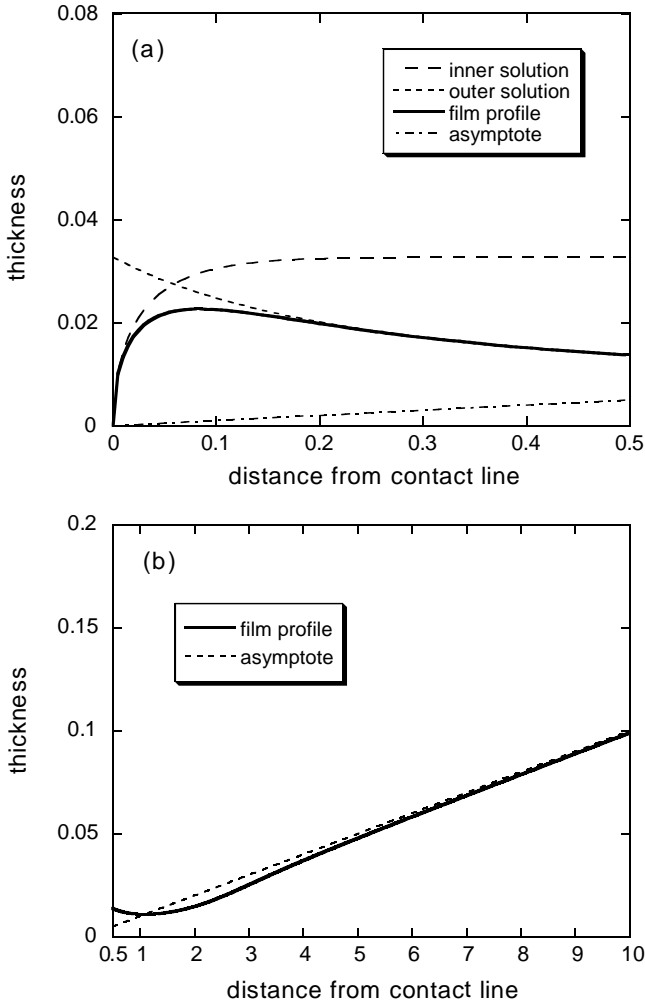
$$z_{2,\text{in}} = \int_0^{e_2} \frac{\tilde{e}\,\mathrm{d}\tilde{e}}{\sqrt{C\,\tilde{e}^3 + 2D\,\tilde{e}^2 + \frac{1}{3}}} \tag{31}$$

(with C and D integration constants).

The lower limit of integration in (31) is set to 0 by the boundary condition (19), while application of (20) brings

$$D = -\frac{1}{3}\frac{V^*J}{V^2}\frac{S}{\gamma} \tag{32}$$

---

[5] Or even from any perturbative expansion in the powers of ϵ.

Fig. 4. Film profile in the complete wetting case, for $\epsilon = 2.3 \cdot 10^{-5}$ and $S/\gamma = 0.2$ (length unit is ℓ on both axes). (a) Vicinity of the contact line. (b) Outer region. After a few ℓ's, the film merges with the macroscopic tilted flow of angle θ (asymptote). Note, in each plot, the very different scales between the two axis: the one giving the distance from the contact line should be considerably stretched to get a representative idea of the actual film profile.

(negative for our wettable surface).

We now proceed to the asymptotic matching [15–18] of the inner and the outer solution[6]. The first-order matching condition writes

$$\lim_{z_2 \to +\infty} e_2(z_2) = \lim_{z_1 \to 0} e_1(z_1). \tag{33}$$

The l.h.s. admits a finite limit only if C takes the specific value

$$C = \frac{2\sqrt{2}}{3}(-D)^{3/2}. \tag{34}$$

The value of this limit is then $e_{\mathrm{p}}/\theta\ell$, where e_{p} is the thickness of the static pancake (Eq. (10)) that the liquid would

---

[6] The following derivation has been inspired by the work of J.-F. Joanny in the related problem of liquid spreading [19].

form at rest on the surface, without aspiration. We then equate this value with the r.h.s. limit of the matching condition, which is equal to $1/K$, and find

$$K = \frac{\theta\ell}{e_{\mathrm{p}}}. \tag{35}$$

The solutions found for the inner (Eq. (31)) and outer (Eq. (27)) regions, together with equations (32), (34) and (35), give us a complete description of the profile of the film over a wettable substrate. Figures 4a and 4b present the profile that is obtained, respectively, in the close vicinity of the contact line, and farther away in the outer region.

Our results call for a few important comments:

i) When plotted in orthonormal coordinates, the liquid takes the shape of a long, almost flat, strip at the approach of the contact line. This is naturally a remembrance of the usual precursor film that is encountered in the wetting process of a (wettable) surface by a drop [9]. In physical units, the thickness of this "tongue" is indeed similar to that of a precursor, both being of order e_{p}[7].

ii) We are now able to give an order of magnitude for the distance over which the flow merges with the simple, non-dissipative, flow of Section 3.2. This merging is described by the outer solution $e_{1,\mathrm{out}}$, and in Figure 4b we see that it occurs over a distance of a few ℓ's (Eq. (24)), that is to say on microscopic scales. Practically, only the macroscopic tilted flow of angle θ is observable, thus validating the simple analysis of reference [6][8].

iii) One question remains: what determines the actual position of the contact line? We know from the previous section that a delicate hydrodynamic balance entails that the contact line necessarily lies on the position obtained by a straight extrapolation of the asymptotic linear profile of angle θ. If this asymptotic line is shifted, then the whole profile is shifted by the same amount, without change: all the positions of the contact line are equivalent. But this degeneracy is naturally broken when we attempt to match the asymptotic profile with the meniscus originating in the bath from which the plate is pulled out. This matching, by fixing the asymptotic line, also determines the contact line position.

3.5 Partially wettable surface

We now consider the situation of a partially wettable surface. In fact, physical intuition encourages us to think that this will not be a mere extension of the wetting case. In the pull-out process, due to aspiration, the contact line is

---

[7] The appearance of a static quantity as e_{p} is not a surprise: in the inner region, the dynamic term was totally ignored. If we increase the dynamic drive (by increasing V), this static approximation can still be made, but the region over which it remains valid ($\sim \epsilon^{1/2}\ell$) diminishes accordingly.

[8] In the limit $J \to 0$, the merging length ($\sim \ell$) increases towards infinity, but one must notice that at the same time $\theta \to 0$ at a faster rate: there is no contact line anymore, and we go back to a classic infinite Landau-Levich film.
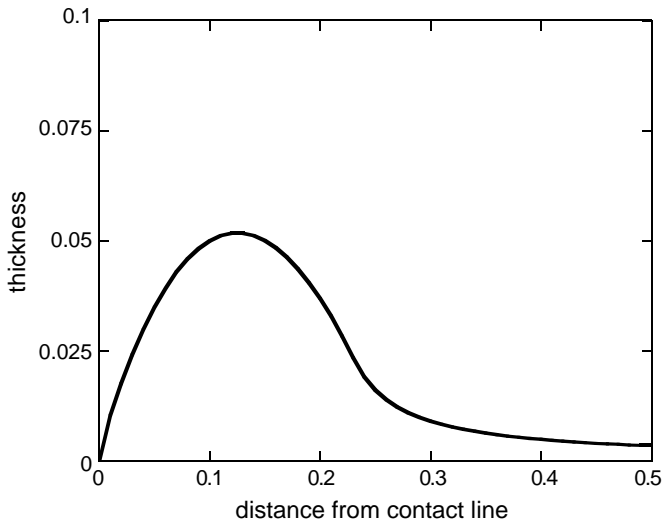
Fig. 5. Film profile near the contact line in the partial wetting case, for $\theta = 10^{-3}$ and $\epsilon = 2.3 \cdot 10^{-5}$ (length unit is ℓ on both axes). The profile presents a "bump" corresponding to the intermediate region. Farther away from the contact line, the profile approaches the asymptote in a way similar to the wetting case (not shown).

Fig. 6. Bump steepening in the film profile (partial wetting) as the pull-out velocity is increased (decreasing values of ϵ).
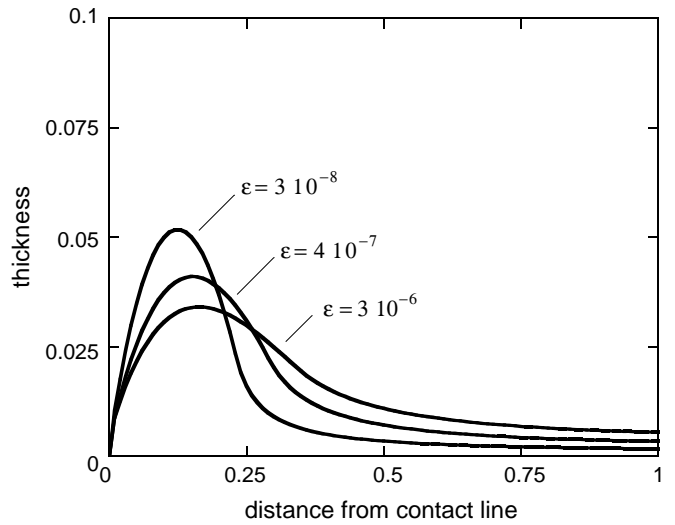
forced to recede on the plate. For a wettable substrate, we have shown that this dewetting occurs with the liquid leaving, just below the contact line, a thin strip similar to a precursor film. On a partly wettable surface, however, the liquid is not inclined to leave any film at all, but rather to adopt a sharp profile which is in obvious contradiction with the asymptotic line of small angle $\theta \ll 1$. How does the system resolve the dilemma?

We analyse this situation along the same lines as previously. In the (z_1, e_1) set of variables (Eqs. (22) and (23)), capillarity is still a singular perturbative term, but is called to be important near the contact line. The solution will consequently still exhibit a boundary-layer structure: the outer solution (Eq. (27)) must be abandoned in the vicinity of the contact line, where the inner solution given by equation (31) takes place.

However, in equation (31), an important change occurs: the constant $D = -\frac{1}{3}(V^*J/V^2)(S/\gamma)$ (Eq. (32)) is now *positive*, because the spreading parameter S is negative in the partial wetting case. We then go on and try to match the inner and the outer solution with the condition (33), but this appears to be impossible: whatever the value of the constant C in the inner solution, the l.h.s. of equation (33) does not admit any finite limit[9].

This mismatch takes its roots in the discrepancy between the behaviour of the profile in the inner region, where it is similar to the steep, hyperbolic profile of a static drop on a partially wettable surface [9], and the outer region where the profile tends to join the low-angle

asymptote. Therefore, a third region, called *intermediate region*, must appear between the inner region and the outer region, so as to bridge the gap.

For the intermediate region to play its role, one is led to keep capillarity, VW and the dynamic term of order one. To achieve this, both the independent and the dependent variables must be scaled with appropriate powers of ϵ. We find

$$z_3 = z/\mu_3, \quad \text{with} \quad \mu_3 = 3^{-1/6}\epsilon^{1/6}\mu_1, \tag{36}$$

$$e_3 = e/\lambda_3, \quad \text{with} \quad \lambda_3 = 3^{1/6}\epsilon^{-1/6}\lambda_1, \tag{37}$$

so that the "intermediate equation" takes the form

$$1 - \epsilon^{1/3}\frac{z_3}{e_3} = e_3^2 e_3''' - \frac{e_3'}{e_3^2}. \tag{38}$$

Deriving an analytical closed-form solution of this strongly non-linear equation reveals to be a difficult task. However, a satisfying approximate solution can be constructed from a linearized form of equation (38), and be matched through a numerical procedure with both the outer and inner solutions to determine all the constants that remained undetermined (yielding values of C and K that are close to 0)[10]. As can be seen in Figure 5, the profile now presents a "bump" that allows a transition between the two extremal regions.

Let us focus our attention on the evolution of this bump when ϵ becomes smaller, for instance when increasing the pull-out velocity V. The length and thickness of the bump are, respectively, of order $\mu_3 \simeq \epsilon^{1/6}\mu_1$ and $\lambda_3 \simeq \epsilon^{-1/6}\lambda_1$. Therefore, compared to the characteristic lengths μ_1 and λ_1 in the outer region, the bump's length shrinks, while, as is shown in Figure 6, it gets steeper because of the negative power of ϵ appearing in λ_3. Such

---

[9] It can be shown that even with the help of more refined matching procedures than that given by equation (33), no matching can be performed between the inner and the outer solution.

[10] For the sake of conciseness, a technical presentation of the procedure [14], unessential to understand the physical picture, has been omitted here.

a steepening appears coherent as an attempt to reconcile conflicting evolutions: when V is incremented, the asymptotic profile flattens more and more ($\theta \to 0$), in increasing contradiction with the "natural" tendency of the profile to display strong slopes in the inner region.

We conclude by pointing out that, as in the wetting case, the merging distance with the macroscopic flow of angle θ is of order ℓ: for practical purposes, there is no visible deviation from the uniformly tilted flow. Indeed, it is an interesting fact that, except for a small region near the contact line where the profile is submitted to the influence of wetting properties (as the spreading parameter), most of the flow is exactly the same in the wetting and the partial wetting case. This is of course to be imputed to the far off-equilibrium issue that we are dealing with: aspiration by the plate forces a contact line to appear in situations where the pull-out is so strong that there should not exist any.

4 Effects of hysteresis

4.1 Pinned, macroscopic, horizontal drop

Let us consider a macroscopic drop on top of the horizontal upper surface of a porous medium with hysteresis. The drop is submitted to a uniform downwards aspiration (current J) while its contact line is strongly pinned ($\theta_r = 0$) at $x = 0$ (the x-axis is along the horizontal surface). Initially, the (macroscopic) profile near the contact line, e, is wedge-like (with a contact angle θ_0): $e(x, t = 0) = \theta_0 x$. How does the profile evolve under the combined effect of aspiration (which would force the contact line to recede) and pinning (which prevents it from doing so)?

In the lubrication approximation, the horizontal velocity field inside the drop writes, using a vertical z-axis:

$$v(x, z) = \frac{U}{e^2}(z^2 - 2ez). \tag{39}$$

This Poiseuille flow is driven by a pressure gradient $\partial p / \partial x$, where $p = -\gamma \partial^2 e / \partial x^2$ (for the macroscopic drop under consideration, van der Waals forces can be ignored, except in a very small region near the contact line).

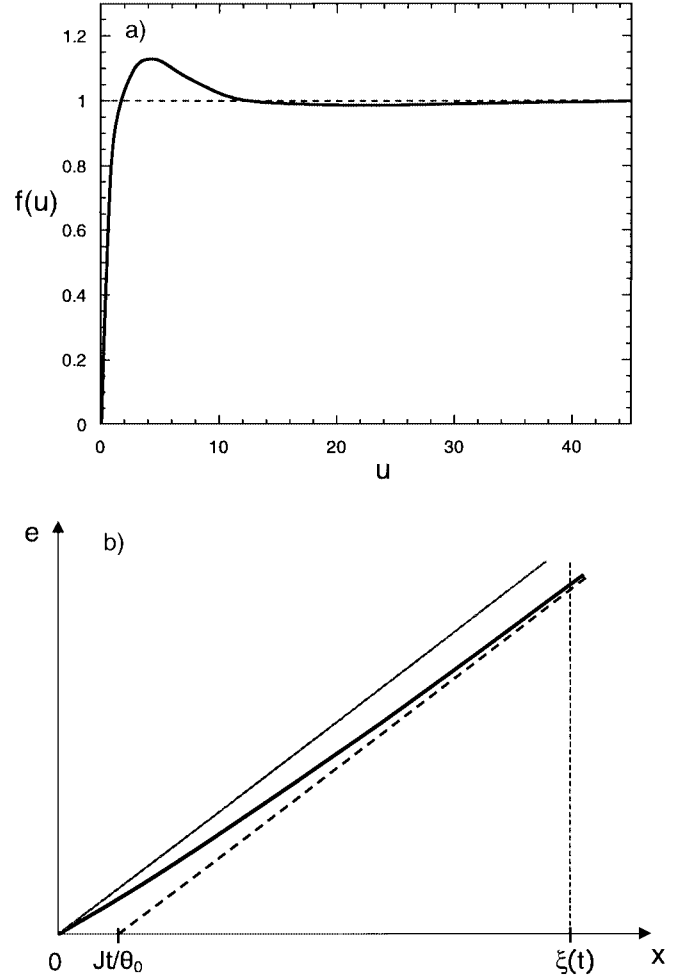Writing $\partial p / \partial x = \eta \partial^2 v / \partial z^2 = 2\eta U / e^2$, we arrive at

$$-\gamma \frac{\partial^3 e}{\partial x^3} = 2\eta \frac{U}{e^2}. \tag{40}$$

The horizontal flow rate, $Q = \int_0^e v(z)\, \mathrm{d}z$, is therefore given by

$$Q = -\frac{2}{3}Ue = \frac{1}{3}V^* e^3 \frac{\partial^3 e}{\partial x^3}. \tag{41}$$

Inserting equation (41) into the conservation equation

$$\frac{\partial e}{\partial t} + J + \frac{\partial Q}{\partial x} = 0, \tag{42}$$

Fig. 7. Macroscopic, pinned, drop under aspiration. (a) Shape of the function $f(u)$ (see text). (b) Deformation of the liquid wedge near the line. The thin solid line represents the initial profile. The effect of pinning is felt inside a region of width $\xi(t)$; beyond, the profile (thick solid line) "heals" and recovers the shape it would have had in the absence of pinning (dotted line).

we find the evolution equation of the profile

$$\frac{\partial e}{\partial t} + J + \frac{\partial}{\partial x}\left(\frac{1}{3}V^* e^3 \frac{\partial^3 e}{\partial x^3}\right) = 0. \tag{43}$$

For a small pumping current J, e remains close to $\theta_0 x$ and equation (43) can be linearized:

$$\frac{\partial e}{\partial t} + J + \frac{\partial}{\partial x}\left(\frac{1}{3}V^* \theta_0^3 x^3 \frac{\partial^3 e}{\partial x^3}\right) = 0 \tag{44}$$

(one can check that the above simplification is actually valid for $J \ll V^* \theta_0^4$).

Far away from the contact line, we expect that the profile is not significantly different from that obtained in the absence of pinning, which would merely be a global downwards translation of the initial wedge by a distance Jt (yielding $e = \theta_0 x - Jt$). It is therefore natural to look

for a solution to equation (44) of the form

$$e(x,t) = \theta_0 x - JtF(x,t), \qquad (45)$$

where the function F describes the effect of the pinning, and is such that, at any given time t, $F(x,t) \sim 1$ for x large enough. We look for a similarity solution $F(x,t) = f(u)$, with a variable u of the form x/t^{α}. Replacement in equation (44) imposes that

$$u = 3\frac{x}{V^*\theta_0^3 t}, \qquad (46)$$

and that f verifies

$$-f(u) + uf'(u) + 1 = \frac{\mathrm{d}}{\mathrm{d}u}\left(u^3 f'''(u)\right). \qquad (47)$$

(The constants in Eq. (46) have been chosen so as to cancel out all physical quantities from Eq. (47)).

Since we require that for $t > 0$, $e = 0$ at $x = 0$, we have the boundary condition $f(u = 0) = 0$. Also, for the reasons exposed above, far away from the contact line, we must have $f(u \to +\infty) = 1$. We finally impose zero horizontal flow at $x = 0$ and $x \to +\infty$.

The behaviour of f is shown in Figure 7a. For $u \to 0$, f is not analytical. For $u \to +\infty$, f presents decreasing oscillations, and behaves like a linear combination of $e^{-(3/2)u^{1/3}}\cos(3(\sqrt{3}/2)u^{1/3})$ and $e^{-(3/2)u^{1/3}}$. $\cdot\sin(3(\sqrt{3}/2)u^{1/3})$. The essential feature of f is that it approximately reaches its asymptotic value ($f = 1$) for u of order unity.

Therefore, we can conclude that the effect of the pinning is felt only in a region of breadth $\xi(t) = \frac{1}{3}V^*\theta_0^3 t$, and that beyond this "healing length", the drop recovers the profile it would have adopted in the absence of contact line pinning. Finally, the initial (macroscopic) contact angle of the drop is slightly reduced during the pumping:

$$\frac{\delta\theta}{\theta_0} \simeq \frac{J}{V^*\theta_0^4} \qquad (48)$$

(justifying in retrospect the linearization of Eq. (43)). The shape of the drop is shown in Figure 7b.

4.2 Pull out with hysteresis

We now return to the modified Landau-Levich problem with the geometry of Figure 3 and we allow for some hysteresis in the contact angle.

We start with the case of *strong pinning*, where the receding angle θ_r is equal to zero. Let us denote $F(V)$ the pinning force felt by the contact line at velocity V. Strong pinning implies that, for a flat macroscopic film, the force required to depin the contact line, equal to $F(V = 0)$, is larger than the capillary force $\gamma_{SL} + \gamma$, see footnote[11]. Formally, this is exactly similar to what we had in our discussion of Section 3.4, with a wettable surface displaying

---

[11] In our notation, the capillary force γ_{SO} has been absorbed in $F(V)$.

no hysteresis and $\gamma_{SO} > \gamma_{SL} + \gamma$. The spreading parameter S should simply be "renormalized" to $\tilde{S} = F(V) - \gamma_{SL} + \gamma$. In the region close to the contact line, the liquid forms a thin strip, with a thickness of the order of the pancake thickness e_p. Here, e_p is defined by the force balance

$$F(V) - \left(\gamma_{SL} + \gamma\right) = P(e_p) + e_p\Pi(e_p). \qquad (49)$$

We do not know much about the velocity dependence of the pinning force $F(V)$ at large V. For simplicity, we shall assume that $F(V)$ is an increasing function of V. Thus $F(V) > F(0)$, and the left-hand side of equation (49) is constantly positive. Hence, equation (49) admits, in principle, a solution $e_p(V)$.

Again e_p is very small, and we expect the visible profile to be dominated by the macroscopic solution: dissipation occurs only within a finite vertical distance ℓ. At greater distances, we return to a uniform flow of tilt angle θ.

Let us now turn to the case of *weak pinning* ($\theta_r > 0$). Here, our pinning force $F(V)$ is weaker at low V:

$$F(0) - (\gamma_{SL} + \gamma) < 0. \qquad (50)$$

But we are dealing with relatively high velocities V at which $F(V)$ may become larger. We are thus led to two possibilities:

a) if $F(V) > \gamma + \gamma_{SL}$, we return to the case of strong pinning.

b) if $F(V) < \gamma + \gamma_{SL}$, we expect a profile similar to what we discussed in Section 3.5 for partial wetting: at the approach of the contact line, the profile thickens, forming a bump.

In both cases, again, the transition to the macroscopic flow occurs on a microscopic region of size ℓ.

5 Concluding remarks

We conclude with the following remarks:

1) A number of interesting experiments are conceivable with a pumped porous medium: for instance, in pull out, measuring the finite height H achieved by a Landau-Levich film. The surprise is that H is dictated by the uniform tilted flow:

$$H \simeq \frac{e_L}{\theta} \simeq e_L\frac{V}{J}, \qquad (51)$$

and is insensitive to the delicate dissipation processes taking place near the triple line: the "near" field is of nanoscopic size for most cases. And in practice, the finite size of the pores may provide a more important cut off than the length ℓ discussed in Sections 3.4 and 3.5.

2) There are interesting questions related to the pinning forces $F(V)$ at large velocities. Here, the contact line is not necessarily the end point of a liquid wedge: it may represent the border between a dry region and a thin pancake. But the application of these ideas to porous media, with pores of finite diameter, seems remote.

3) If we want to avoid these difficulties, we can think of pumping a liquid droplet, on a non-porous surface, by

evaporation: this was indeed the starting point of a series of experiments by the Chicago group [20]. We benefit from having a smooth solid surface. But evaporation has its own complications: temperature gradients induce Marangoni flows, which are complex and not very instructive.

4) Returning to the pull out problem, we should also insist on another limitation of our discussion: we restricted ourselves to steady state regimes. At high velocities, the liquid wedge might decide to emit a periodic train of droplets (or pancakes): these droplets would then be pumped out by the current J. A tap delivering a low output of water is a good example of periodic droplet emission. This idea is attractive. However, because of the nanoscopic size of the objects involved, the effects may be hard to observe.

References

1. F. Brochard-Wyart, P.G. de Gennes, Adv. Colloid Interface Sci. **39**, 1 (1992).
2. A. Buguin, L. Vovelle, F. Brochard-Wyart, Phys. Rev. Lett. **83**, 1183 (1999); A. Buguin, Ph.D. thesis, Université Paris 6, Paris (1998).
3. P.G. de Gennes, C. R. Acad. Sci. (Paris), Ser. II B **318**, 1033 (1994).
4. L. Landau, B. Levich, Acta Phys. Chem. (USSR) **17**, 42 (1942).
5. D. Quéré, A. de Ryck, Ann. Phys. (Paris) **23**, no. 1, 1 (1998).
6. E. Raphaël, P.G. de Gennes, C. R. Acad. Sci. (Paris), Ser. II B **327**, 685 (1999).
7. J.R. Philip, Ann. Rev. Fluid Mech. **2**, 1777 (1970).
8. L. Bacri, F. Brochard-Wyart, to be published in Eur. Phys. J. E.
9. P.G. de Gennes, Rev. Mod. Phys. **57**, 827 (1985).
10. F. Brochard-Wyart, J.M. di Meglio, D. Quéré, P.G. de Gennes, Langmuir **7**, 335 (1991).
11. B.V. Derjaguin, *Theory of Stability of Colloids and Thin Films* (Consultants Bureau, New York, 1989).
12. F. Brochard-Wyart, J. Daillant, Can. J. Phys. **68**, 1084 (1990).
13. P.G. de Gennes, X. Hua, P. Levinson, J. Fluid Mech. **212**, 55 (1990).
14. A. Aradian, E. Raphaël, P.G. de Gennes, in preparation.
15. C. Bender, S. Orszag, *Advanced Mathematical Methods for Scientists and Engineers* (McGraw-Hill, Singapore, 1978).
16. M. Van Dyke, *Perturbation Methods in Fluid Mechanics* (Academic Press, New York, 1964).
17. A. Nayfeh, *Perturbation Methods* (Wiley and Sons, New York, 1973).
18. J. Kevorkian, J. Cole, *Multiple Scale and Singular Perturbation Methods* (Springer Verlag, New York, 1996).
19. J.-F. Joanny, J. Méc. Théor. Appliquée, No. Spécial **249** (1986).
20. R. Deegan, O. Bakajin, T. Dupont, G. Huber, S. Nagel, T. Witten, Nature **389**, 827 (1997).